7131/97

Broadband Plasma Waves Observed in the Polar Cap Boundary Layer (PCBL) : POLAR

B. T. Tsurutani, C. M. Ho, G. S. Lakhina,
A. Boonsiriseth, and J. K. Arballo
Jet Propulsion Laboratory, Pasadena, CA 91109

J. S. Pickett and D. A. Gurnett
The University of Iowa, Iowa City, IA 52242

W. K. Peterson
Lockheed Space Science Laboratory
Palo Alto, CA 94304

R. M. Thorne
University of California Los Angeles, CA 90024

Abstract. Polar observations indicate the presence of intense broadband plasma waves nearly all of the time (-100% occurrence frequency during this study) near the apogee of the Polar trajectory (-6-8 Re). The region of wave activity bounds the dayside (05 to 18 LT) polar cap magnetic fields, and we thus call these waves Polar Cap Boundary Layer (PCBL) waves. The waves are spiky signals spanning a broad frequency range from -101 to 2 x 10^4 Hz. The waves generally have a power law spectral shape. The wave magnetic component has on average a f‘27 frequency dependence and has an upper frequency cutoff of -(6-7) x 10^3 Hz, which is the electron cyclotron frequency. The electric component has on average a f ‘^{2}2 frequency dependence and extends up to -2 x 10^4Hz. The frequency dependence of the waves and the amplitude ratios of B ‘/E’ indicate a possible mixture of obliquely propagating electromagnetic whistler mode waves plus electrostatic waves. There are no clear intensity peaks in either the magnetic or electric spectra which can identify the plasma instability responsible for the generation of PCBL waves.

The wave character (spiky nature, frequency dependence and admixture of electromagnetic and electrostatic components) and intensity are quite similar to those of the low latitude boundary layer (LLBL) waves detected at and inside the low latitude dayside magnetopause. Due to the location of the PCBL waves just inside the polar cap magnetic field lines, it is natural to assume that these waves are occurring on the same magnetic field lines as the LLBL waves, but at lower altitudes. Because of the similar wave intensities at both locations and the occurrence at all local times, we rule out an ionospheric source. We also find a magnetosheath origin improbable. The most likely scenario is that the waves are locally generated by field-aligned currents or current gradients. We find a strong relationship between the presence of ionospheric and magnetosheath ions and the waves near the noon sector. These waves may thus be responsible for ion heating observed near the cusp region.

INTRODUCTION

Broadband plasma waves have been detected within the Earth's magnetopause low latitude boundary layer (LLBL) by the ISEE- 1 and -2 [*Gurnett et al., 1979; Tsurutani et al.,* 1981; 1989; *Anderson et al., 1982],* GEOS [*Gendrin*, 1983; *Rezeau et al.,* 1989; *Belmont et al., 1995]* and AMPTE [*LaBelle and Treumann*, *1988]* spacecraft. Similar waves have been detected and characterized at the Jovian (rnagnetopause) low latitude boundary layer [*Tsurutani et al.*, *1993; 1997].* These boundary layer waves have been demonstrated to be sufficiently intense to cause cross-field diffusion of magnetosheath plasma to form the boundary layer itself at both Earth and Jupiter [*Tsurutani and Thorne*, *1982; Tsurutani et al., 1997].* If this mechanism is indeed in effect at the magnetopause, then the waves play an important role in the transfer of energy from the solar wind to the magnetosphere. This cross-field diffusion of particles, energy and momentum would be one form of viscous interaction between the solar wind and the magnetosphere [*Axford and Hines,* 1961; *Tsurutani and Gonzalez,* 1995].

It is the purpose of this paper to report the first results of a search for waves on similar magnetic field lines as the LLBL, but using the POLAR spacecraft which has an apogee of only -9 Re, a much smaller distance than the magnetopause distance. In Figure 1, we show the POLAR orbit, which has a high inclination and is covering the noon-midnight sector. Under ordinary circumstances the POLAR spacecraft does not intercept the magnetopause [*Pickett et al.,* 1997], but as shown from the diagram, the spacecraft does cross field lines that map into the LLBL. It is the search for waves in these field regions (6 to 8 Re from Earth) that is the focus of this paper. In this paper, we will concentrate our efforts on the dayside region only.

The generation mechanism of the LLBL waves is not well understood. Some suggested mechanisms are the lower hybrid drift instability *[Gary and Eastman*, 1979; *Hubs et al.*, 198 1] driven essentially by the density gradients, the electron loss cone instability driven by velocity space gradients [*Kennel and Petschek*, *1966],* velocity shear and drift instabilities [*Lakhina,* 1987; *1993*; *Lakhina et al.,* 1995], and a magnetic shear instability [*Zhu et al.,* 1996]. The emissions arc broadbanded with no obvious spectral peaks which could be used to identify particular instabilities. An electrostatic current convective instability [*Drake et al.,* 1994a] and a whistler instability *[Drake et al.,* 1994b; 1995] driven unstable by the gradient of the field-aligned currents, with an evolution to a

turbulent state have been proposed. Through a comparison of wave intensities observed at POLAR to previous measurements by ISEE, GEOS and AMPTE and of the ratio of B'/E' to determine the wave mode(s), we hope to gain further information to help identify possible generation mechanisms/free energy sources.

We also examine the energetic (-O, 1 to 10 keV or higher) ion fluxes as detected by the toroidal imaging mass-angle spectrograph (TIMAS) experiment on POLAR to determine if there is a relationship between ions and the waves. The details about the TIMAS experiment are given in Shelley *et al.* [1995]. Enhanced fluxes of H+, He^{++} and 0^{+} ions are observed to be correlated with the intense wave events.

METHOD OF ANALYSES

The Polar spacecraft and its electric dipole antennas, magnetic loop antenna, and triaxial search coil antennas are indicated in Figure 2. The three orthogonal electric dipole antennas, E_U, E_v, and E_Z, have tip-to-tip lengths of about 130 m, 100 m, and 14 m, respectively, and are used to detect the ac electric fields. Two of these electric antennas are mounted in the spin plane of the spacecraft, E_u and E_v, and one is aligned along the spin axis, E_Z. The magnetic loop antenna, L, which consists of a single loop of aluminum tubing with 1.0 m^2 area, and the three orthogonal magnetic search coil antennas, B", B_v, and B_z, each with 20,000 turns of No. 40 wire, are mounted on the end of a 6-m rigid boom and are used to detect ac magnetic fields. The magnetic loop senses along the same direction as the electric E_U antenna. The search coil antennas, B_U, B_V, and B_Z, sense along the corresponding directions of the electric antennas, E_u, E_v, and E_Z, respectively.

We first identify wave intervals of interest by use of frequency-time spectrograms of the electric and magnetic field components of the waves which are obtained by two different types of plasma wave receivers. The Sweep Frequency Receiver (SFR) consists of two single-sideband, phase-matched, double-conversion receivers in parallel, and are referred to as SFR-A and SFR-B (the "A" and "B" designators have no significance other than for distinguishing between the two receivers). The SFR provides good frequency resolution (about 8% at 26 Hz and 3% at 800 kHz in log-step mode) with relatively poor time resolution (one full frequency spectrum every 32 s in the log-step mode or every 64 s in the linear-step mode). The Multichannel Analyzer (MCA) consists of two spectrum analyzers, and are referred to as MCA-E and MCA-B (the "E" and "B" designators are used only to

distinguish between the two receivers). The MCA provides good time resolution (one full frequency spectrum every 1.3 s) with relatively poor frequency resolution (4 frequency channels per decade). For more detailed information on these receivers and the antennas that are used to detect the wave signals, please refer to the Plasma Wave instrument (PWI) description contained in *Gurnett et al. [1995].*

The Polar orbit has an ~86° inclination with an apogee of ~9 R_E and a perigee of ~1.8 R_E. The orbital period is about 18 hours. At the beginning of the mission, the Polar apogee was set over the northern polar region. The location of the spacecraft is identified by orbital parameters (radial distance, magnetic local time and eccentric dipole L-shell value) obtained from Polar predictive and definitive obit data, and through the use of the Tsyganenko T89 model with Kp=3-, 3 and 3+ options. At this stage of our analysis, the true geomagnetic activity has not been taken into account.

RESULTS

A frequency-time color spectrogram of the data obtained on April 7, 1996 from the Polar PWI Multichannel Analyzer while switched to the 130 m electric antenna located in the spin plane is shown in Figure 3. This plot covers 24 hours as shown along the horizontal axis, and a frequency range of 5 Hz to 311kHz, the MCA-E's full frequency range, as shown along the vertical axis. The electric field power spectral density is plotted according to the color bar to the right of the spectrogram. The spacecraft event time (SCET), which corresponds to Universal Time, radial distance from the center of the earth (R_E), magnetic latitude (λ_M), magnetic local time (MLT), and approximate L-shell value, are indicated at the bottom of the plot.

On this day, Polar was first at its perigee around the south pole at 0140 UT, corresponding to a very high magnetic field strength and electron cyclotron frequency $>10^5$ Hz. It next passed through the dayside plasmasphere/magnetosphere at ~0300 UT. Strong whistler mode waves (hiss and chorus) were detected in this latter region. At 0445 UT the spacecraft entered the northern hemisphere polar cap region by crossing the cusp and polar cap boundary layer. Inside the polar cap region we also see some bursty waves, but these are relatively weak. These polar cap wideband waves have an obvious upper cut-off frequency which corresponds to narrowband electron cyclotron emissions [*Gurnett and Frank,* 1978]. At the midpoint of the polar cap (orbit apogee), both the plasma frequency

and electron cyclotron frequency reached their lowest values. Many aurora! kilometric radiation (AKR) events can also be noted inside the polar cap region at frequencies above 10^5 Hz. At 1450 UT, Polar moved from the polar cap to again cross a region of intense broadband waves, but on the nightside. The spacecraft next entered the nightside plasmasphere and started another cycle. The waves seen at about 2130 UT are again the dayside PCBL waves. The waves seen from 0100-0200 UT and 1830-1930 UT are associated with the Polar spacecraft crossing the southern aurora] zones and polar cap. Finally, the intense signals seen beginning at around 0000, 0200, 1730, and 1930 UT are not naturally-occurring plasma waves but rather a manifestation of antenna preamplifier oscillation as the spacecraft passes through the high density plasmasphere region.

The wave intervals of interest are indicated by two sets of arrows along the time axis, and are designated as "Dayside PCBL" and "Nightside PCBL" within the figure. These intervals of intense waves bound magnetic fields that map into the polar cap region. Both wave events occur in the northern hemisphere near apogee. The dayside PCBL event occurs near 13.0 MLT and the other near 0.3 MLT, as the spacecraft orbit is in a near noon-midnight orientation.

The PCBL waves are characterized by bursts of turbulence covering a broad frequency range extending from $f < 10^1$ to 2×10^4 Hz as shown in the MCA electric field spectrum of Figure 3. The MCA best illustrates this nature of the waves since it has good time resolution and is not concerned with narrowband frequency resolution. The magnetic field spectrum for these waves shows similar type bursts. However, the intensity of the magnetic component of the waves is much nearer the background level of the receiver. Therefore, the magnetic component is harder to discern in spectrogram format and is not presented here in that form. The region between the dayside PCBL and the nightside PCBL (about 0555 to 1450 UT) is identified as the northern polar cap. In this region there is typically a lack of strong signals although a few bursts of electrostatic noise are seen, as well as auroral hiss ($\lesssim$3 kHz) and aurora] kilometric radiation ($\gtrsim$100 kHz). The vertical lines seen at about 1100 UT are an instrument artifact caused by crosstalk from the SFR as it switched from logarithmic to linear mode.

Figure 4 shows the fractional amount of time that the waves are present on the dayside northern hemispherical pass. Using the PWI SFR-A E_U plots, a wave "event" is marked by a start and stop times identified by an observed increase in intensity against background intensity and a subsequent decrease. Our cutoff criterion was approximately 10^{-10}

$(mV/m)^2$, determined by visual inspection of color spectral plots. The start and stop times were tabulated, as well as the spacecraft's location. For each hourly bin, the number of passes are indicated, as well as the number of times PCBL waves were. detected. The Poisson statistics are noted. The interval of analysis was March 13, 1996 to August 31, 1996. Every orbital pass was used and each pass was counted as only one event (228 passes). The plot shows that between 5 and 18 LT for this study, enhanced waves were present 100% of the time.

The display of the geomagnetic latitude of the footpoint of the B-field line passing through the spacecraft versus geomagnetic local time for the events in Figure 4, are given in Figure 5a. In the latter figure we use a magnetic local time resolution of one hour and a latitude resolution of 2 degrees. For each northern hemisphere dayside pass, and for each box the spacecraft passed through, we determine whether waves were present or not. If present, we count this as an event. The figure shows a general display of the location of where the waves are located. The waves map into a relatively narrow band of latitudes from 70° to 85°. This range gives the polar cap boundary layer location, There is a trend for the PCBL waves to extend to slightly lower latitudes in both the dawn and dusk sides relative to the noon sector. Figure 5b shows the corresponding L-values of the wave region versus geomagnetic local time. It is clear that PCBL waves observed on the dayside northern hemisphere occur predominantly in the region with $L \geq 10$.

Wave power spectral densities have been studied for several PCBL events selected at random. Figures 6 and 7 show the electric and magnetic spectra of the two events occurring near the apogee in the northern hemisphere. A hand fit to the data has been drawn and the values for the fits are indicated in the graphs. The background (instrument) noise levels are also indicated for reference. The electron cyclotron frequency is indicated at the bottom of each figure. These latter values are calculated using the onboard magnetometer data [*Russell et al.*, 1995]. The event shown in Figure 6 occurs on day 98, 1996 at 1302 MLT at 78.8° N invariant magnetic latitude. The wave frequency of the electric component extends to -2×10^4 Hz (Fig. 6a), and that of the wave magnetic component extends to -3×10^3 Hz (Fig. 6b). The Figure 7 event occurs on day 114, 1996 at 1235 MLT at 76.3° N invariant latitude. The wave frequency for the electric component extends to -10^4 Hz (Fig. 7a) and that of the corresponding magnetic spectra extends to -5×10^3 Hz (Fig. 7b). Note that the electric component of the waves extends to frequencies above the electron cyclotron frequency.

We have also examined the power spectra for the electric and magnetic components for the event near the Polar perigee in the southern hemisphere (not shown here). This event occurs on day 103, 1996 at 1353 MLT and invariant latitude 73.1 “S. The frequencies of the electric spectrum extend to about 10^5 Hz and those of the magnetic spectrum to about 2 x 10^4 Hz. The wave intensities for this event are comparable to the two apogee events shown in Figures 6 and 7. This will be discussed later.

The spectral density plots for all the events discussed above have rough power-law shapes. The intensities and spectral shapes vary from event-to-event, but generally follow a power law. The E’ waves clearly are present from -101 Hz (the lowest frequency shown) to -2 x 104 Hz for the apogee events. There are signals above this frequency but the results are less clear because the signal strength becomes close to the instrument noise level. The magnetic signals are broad-banded and extend from -10^1 Hz to the electron cyclotron frequency (6-7 x 10^3 Hz) with a fitoff27 in power spectra, on average.

High time resolution wideband receiver (WBR) data for the event occurring on day 114, 1996 are shown in Figure 8. In this figure we have plotted 44 minutes from0616 to 0700 UT on the horizontal axis versus frequency from O to 12 kHz on the vertical axis with color indicating the intensity of the signals. During this time, the WBR is switched to the electric Eu antenna and sampling data at the rate of 31.1 kHz. The data are formatted into a digital data stream and telemetered directly to a ground tracking station rather than tape recorded and telemetered to the ground at a much lower rate. Thus, the WBR provides both good frequency resolution, assuming the appropriate bandpass filter has been chosen for the emission, and also excellent time resolution. In Figure 8, we note that the PCBL waves are very bursty. Around 0630 UT the waves extend up to 10 kHz, but the strongest part appears mainly below 4 kHz. We also note electron cyclotron emission falling from about 7 kHz at 0630 to 6 kHz at 0700. These. overall results are generally consistent with the results from the other portion of the PW instrument presented previously.

These broadband waves clearly have both a magnetic and an electric component. To try to identify the mode of propagation, we determine the B′/E′ ratio for the events of Day 98 and 114, 1996, respectively for the two events shown in Figures 6 and 7. In panels a) and b) of Figure 9 we show the B’/E’ ratio for the events of Day 98 and 114, 1996, respectively.

The calculated refractive indices for the parallel propagating whistler waves in a cold uniform plasma has been added as a reference to the Figure. The cold plasma density data used to derive the refractive indices were obtained from the Polar EFI experiment [*Harvey et* al., 1995, *Mozer*, private communication, 1997]. Density values used are derived from a graph of measured spacecraft potential versus measured density that was collected from earlier spacecraft. The density values obtained in this manner fluctuated considerably during the wave events. For example, N_e values varied from 0.7 to 3.8 cm^{-3} for day 98, and 0.9 to 6 cm^{-3} for day 114. The above density values may have an uncertainty by a factor of 2. We have used the maximum value of N_e in computing the whistler refractive indices. Since the electron plasma frequency is proportional to $\sqrt{N_e}$, the B'/E' ratio may be high by -40%. This is negligible compared to the orders of magnitude variations in the actual values.

For the two events, the B′/E′ ratio generally fits the whistler curve at the lowest frequencies but not at mid-and high-frequencies. Thus, it is possible that there is some (off-axis) refraction associated with the higher frequency components. Since the refractive index for the oblique whistlers varies as $\cos^{-1/2}\theta$ (θ being the angle of propagation relative to magnetic field direction), the refractive index will increase with an increase in θ. Therefore, the higher observed B′/E′ values as compared to parallel whistler curve can be explained by assuming that the waves at mid (100 to 1000 Hz) and high (>1000 Hz) frequencies are propagating obliquely to the magnetic field, It is possible that the PCBL region of enhanced plasma density acts as a wave guide and permits off-axis propagation with a minimum of wave damping. However, modeling such effects would require significant effort and is beyond the scope of (he present work. The B '/E' ratios lie in the range of 10 to 100. Thus, the wave phase velocities range from 3×10^8 to 3×10^9 cm s-[. These velocities are much higher than plasma convection speeds measured in this region of space, so Doppler shift effects on the phase velocities or on the B′/E′ ratios should be negligible.

From Figure 1 we had noted that these PCBL waves occur on field lines that map into or close to the LLBL field lines. The wave characteristics presented here are also quite similar to those of the LLBL waves. In Table 1 we make an intercomparison between the Polar wave power spectra illustrated in this paper and the LLBL waves as measured by

ISEE- 1 and 2 and GEOS. We note that the GEOS event was much more intense than either IS EE- 1 and -2 or Polar wave intensities. However, this event was somewhat anomalous because the spectra were taken when the rnagnetopause was pushed in to the spacecraft orbit (6.6 R_e), and a magnetic storm was ensuing. In addition, GEOS magnetic and electric sensors picked up the electromagnetic signals in the ultra-low-frequency (-O-10 Hz) range. It is possible that the extraordinarily high solar wind ram pressure and intense southward interplanetary magnetic field B_s may have led to unusually high wave power. Such LLBL wave intensity dependence on interplanetary parameters have been discussed at Earth and Jupiter by *Tsurutani et al. [1989]* and *Tsurutani et al. [1997],* respectively. Table 1 also lists a spectrum for day 103, 1996 for POLAR when it was near the southern hemisphere dayside perigee. We note that the wave intensities are of the same order as the high altitude northern hemispherical events.

Figure 10 and 11 show PW1 broadband plasma waves and simultaneous ion fluxes (from the TIMAS experiment) for April 7 (day 98) and April 22 (day 113), 1996. The observed energetic ion populations have features typical of the mid-altitude cusp *[Peterson,* 1985]. Prior to 0500 UT on April 7, and about 1240 UT on April 22, the energy and angular (not shown) distributions of the ions reveal primarily hot quasi-isotropic ion populations characteristic of the dayside magnetosphere. The energy -latitude(time) dispersion in the H^+ and He^{++} populations beginning about 0505 and 0530 UT on April 7 and about 1242 UT on April 22, are characteristic of the entry of magnetosheath plasma in the cusp or boundary layer. The regions of most intense wave activity (0500 to0515 UT on April 7 and -1240 to 1250 UT on April 22) are associated with significant changes in the angular distributions in the upflowing 0^+ ions. Specifically, in these regions, the upflowing, relatively low energy 0^+ ions have angular distributions that are peaked at 50 to 70 degrees relative to the magnetic field direction. They have energies of a few hundred eV. The TIMAS instrument was operated in a mode with limited angular resolution for He^+ ions during these intervals. We are not able to determine if the observed upflowing He^+ ion distribution is characterized by a conic angle larger or smaller than the one that characterizes the 0^+ distributions.

The most probable mechanism for which the 0^+ ions can gain significant energy transverse to the local magnetic field is through interactions with waves. Assuming that heating occurs primarily in the perpendicular direction, we can estimate the location of the region below the spacecraft. Because the magnetic field strength falls off roughly as r^{-3} and the first adiabatic invariant ($E_\perp/B$) is conserved (where $E_\perp$ is the perpendicular

energy), we can estimate the maximum distance below the spacecraft where the transverse energy was possibly acquired, For conic angles of 50, 60, and 70 degrees at an altitude typical for these observations (5.5 R,), the maximum distances below the spacecraft where the transverse energy could be acquired are 0.9, 0.5, and 0.2 Earth Radii (R_e), respectively, This is quite close to the spacecraft location.

A systematic examination of the occurrence of these intense waves at the polar cap boundary at local times near dawn and dusk has shown that if upflowing 0^+ ions are present at the time of these waves, the 0^+ distribution has a characteristic conic angle indicating that significant transverse energy was acquired up to 1 Re below the spacecraft. We note that there were intervals where intense waves were present, but no discernible upflowing 0^+ ions were observed. The appearance of transversely energized 0^+ ions simultaneous with enhanced wave intensity indicates that there is a strong possibility of near-local heating of the ions by the waves. However this is beyond the scope of the present paper, and another effort is in progress to address this issue.

SUMMARY

Below are some of the main findings with regard to the PCBL waves:

1) The PCBL waves are present nearly all of the time on the dayside (between 05 and 18 LT) at 6 to 8 R_e in the POLAR orbit.

2) The waves are located at 70” to 80° invariant magnetic latitude. This location is just below the cusp fields (75° to 85° latitude, Russell, personal communication, 1997) and thus corresponds to LLBL field lines.

3) There is both an electric and a magnetic component to the waves where the electric component extends from -10 Hz to 2 x 10^4 Hz and the magnetic from -10 to 5 x 10^3 Hz.

4) The emissions are bursty, but when viewed over longer time intervals, they fit a general power law with a f‘22 dependence for E’ and f”27 dependence for B’ waves, on average.

5) The B ‘/E’ ratio is consistent with the parallel propagating whistler mode waves for the low frequency (10’- 10^2 Hz) component. However, the B’/E’ ratio is often higher at mid-

(10^2 - 10^3 Hz) and high- (10' to 6 x 10^3 Hz) frequencies, consistent with off-axis propagating waves.

6) The waves have very similar intensities, spectral shapes and E' and B' dependence as the LLBL waves. The PCBL waves are similar to the broadband noise on the auroral field lines [Gurnett and Frank, 1977; Gurnett et al., 1984] but unlike the latter, the PCBL waves do not have any clear peaks at any frequency.

7) The intense noon sector wave events are well correlated with enhanced fluxes of 10 to 200 eV H+, He^{++} and 0^{+} ions.

DISCUSSION AND CONCLUSION

Because the PCBL waves are quite similar to the LLBL waves, we assume that they are on the same magnetic field lines. A schematic of these field lines, the PCBL wave locations and the LLBL wave locations are shown in Figure 12. Although to date such waves have been identified at only three regions along the field lines (PCBL, LLBL and near Polar perigee), one can argue that the waves most likely exist along the entire length of the field lines. Here we have assumed that the field lines are "closed" and extend from one hemispherical ionosphere to the other.

The PCBL wave field lines must be configured as indicated in Figure 12, where they map into the earth's ionosphere over a broad region of local times. Because the northern hemispherical waves are detected at only 6 to 8 Re from the Earth on relatively strong fields, the chance they map into the cusp region is highly improbable. *Russell* (personal communication 1997) has reported that the Polar magnetometer (statistically) detects cusp field lines at slightly higher latitudes and that the cusp only extends ±2 hours from local noon at Polar altitudes.

The three point intensity (LLBL, Polar near-apogee, Polar near perigee) measurements give strong constraints on the wave source location. If wave generation occurs in the ionosphere, upward wave propagation would lead to wave intensity decreases by orders of magnitude due to flux tube expansion alone. Wave damping and scattering would decrease intensities further. Thus, we can rule out an ionospheric source. Another possibility that has been discussed in the literature is that magnetosheath magnetosonic

waves have coupled into LLBL Alfvén waves [*Johnson and Cheng*, 1997] or they are magnetosheath waves that have been amplified at the magnetopause and propagated down the magnetic field lines [*Belmont et al.*, 1995]. This possibility also seems unlikely in view of the new results. If this were the case, then one would expect waves to be located primarily at noon with little or no waves present at the PCBL dawn and dusk flanks. One should note, however that the waves are slightly higher in intensity at noon than at dawn and dusk. Moreover, this wave-coupling mechanism would work only for ultra-low-frequency (ULF) waves which are much below the PCBL broadband plasma wave frequencies.

The most likely scenario is wave generation by a local source of free energy existing along field lines. Two possible sources are field-aligned currents and density gradients. *Drake et al. [1994a,* b] have proposed current convective and whistler instabilities driven by the gradient of the field-aligned current as a possible mechanism for the generation of broadband plasma waves in the magnetopause current layer. Our preliminary theoretical analysis indicates that the presence of density gradients tends to stabilize both the current convective and whistler instabilities in the sense that their growth rates are reduced, and somewhat higher current gradients are needed to excite these modes [*Lakhina* et *al.,* 1997]. However, the density gradients introduce a finite real frequency to the current gradient driven modes. On the other hand, when the ions are hot, the lower hybrid drift instability can be excited provided the density gradients are sharp (- ion gyro radii) [*Gary and Eastman,* 1979; *Hubs et al.,* 1981; *Bhatia and Lakhina, 1980].* Weaker density gradients can excite drift modes [*Lakhina et al., 1995].* However, these modes correspond to ULF waves which occur at much lower frequencies than that of the PCBL broadband plasma waves discussed here.

The plasma and field results taken from this data set are currently being used to model instabilities of these types. In addition, hot plasma ray tracing models are being employed to examine the electromagnetic and electrostatic wave transport properties in this region of space. The density enhancements in the PCBL will act as "ducts" or wave guides for the waves. Also the plasma density gradient at the magnetopause, density gradients at the inner edge of the PCBL, and field curvature, will play strong roles in the wave propagation characteristics. Since the intense wave energy correlates with enhanced fluxes of energetic ions, interaction of these waves with the ions is expected to play an important role in the processes which lead to heating/acceleration of H^+, He^{++} and 0^+ ions [*Chang and Coppi*, 1981; *Roy and Lakhina*, 1985; *Andre et al., 1990; Crew et al, 1990; Lakhina*, 1993;

Lakhina and Buti, 1996]. The broadband plasma waves could precipitate energetic electrons and ions into the loss cone, leading to the excitation/enhancement of the auroral intensities.

Acknowledgments:. Portions of this paper represent work done at the Jet Propulsion Laboratory, and the California Institute of Technology, Pasadena, under contract with the National Aeronautics and Space Administration and under subcontract with the University of Iowa. J. S. Pickett and D. A. Gurnett acknowledge the support of NASA under NASA/GSFC Contract No. NAS 5-30371. We thank C. T. Russell for providing Polar magnetic field data. Work at Lockheed Martin was supported by NASA Contract No. NAS 5-33032. F. Mozer would like to acknowledge NASA Contract NAS 5-30367 and grant NAS 5-3182 for support of portions of this effort. G. S. Lakhina would like to thank National Research Council for the award of a Senior Resident Associateship at Jet Propulsion Laboratory.

References

Anderson, R. R., C.C. Harvey, M.M. Hoppe, B.T. Tsurutani, T.E. Eastman, and J. Etcheto, Plasma waves near the magnetopause, *J. Geophys. Res.*, 87,2087, 1982.

Andre, M., G.B. Crew, W.R. Peterson, A.M. Persoon, C.J. Pollock, and M.J. Engebretson, Ion heating by broadband low-frequency waves in the cusp/cleft, *J. Geophys. Res., 9S,* 20809, 1990.

Axford, W. I., and C.O. Hines, A unifying theory of high-latitude geophysical phenomena and geomagnetic storms, Can. *J. Phys.*, 39, 1433, 1961.

Belmont, G., F. Reberac, and L. Rezeau, Resonant amplification of magnetosheath MHD fluctuations at the magnetopause, *Geophys. Res. Lett.*, 22, 295, 1995.

Bhatia, K. G., and G.S. Lakhina, Drift loss cone instability in the ring-current and plasmasheet, *Proc. Indian Acad. Sci. (Earth Planet Sci.), 89,99,* 1980.

Chang, T., and B. Coppi, Lower hybrid acceleration and ion evolution in the supra-auroral region, *Geophys. Res. Lett., 8, 1253,* 1981.

Crew, G. B., T. Chang, J.M. Retterer, W.K. Peterson, D.A. Gurnett, and R.H. Huff, Ion cyclotron resonance heated conies: Theory and observations, *J. Geophys. Res.*, 9.5, 3950, 1990.

Drake, J. F., J. Gerber, and R. G. Kleva, Turbulence and transport in the magnetopause current layer, *J. Geophys. Res.*, 99, 1 I 211, 1994a.

Drake, J. F., R. G. Kleva, and M.E. Mandt, Structure of thin current layers: Implications for magnetic reconnection, *Phys.* Rev. *Lett.*, 73, 1251, 1994b.

Drake, J. F., Magnetic reconnection, a kinetic treatment, in *Physics of the Magnetopause*, Geophys. Mon. 90, Amer. Geophys. Union, Washington, D. C., 155, 1995.

Gary, S.P. and T.E. Eastman, The lower hybrid drift instability at the magnetopause, *J. Geophys. Res.*, 84,7378, 1979.

Gendrin, R., Magnetic turbulence and diffusion processes in the magnetopause boundary layer, *Geophys. Res. Lett., 10,769, 1983.*

Gurnett, D. A., and L.A. Frank, A region of intense plasma wave turbulence on auroral field lines, *J. Geophys. Res.*, 82, 1031, 1977.

Gurnett, D. A. and L.A. Frank, Plasma waves in the polar cusp: Observations from Hawkeye, J. *Geophys. Res.*, 83, 1447, 1978.

Gurnett, D. A., R.R. Anderson, B.T. Tsurutani, E.J. Smith, G. Paschmann, G. Haerendel, S.J. Bame, and C. T'. Russell, Plasma wave instabilities at the magnetopause: Observations from ISEE 1 and 2, *J. Geophys. Res.*, 84,7043, 1979.

Gurnett, D. A., R.L. Huff, J.D. Menietti, J.L. Burch, J.D. Winningham, and S.D. Shawhan, Correlated low-frequency electric and magnetic noise along the auroral field lines, *J. Geophysical Research*, 89,8971, 1984.

Gurnett, D. A., A.M. Persoon, R.F. Randall, D.L. Odem, S.L. Remington, T.E. Averkamp. M.M. Debower, G.B. Hospodarsky, R.L. Huff, D.L. Kirchner, M.A. Mitchell, B.T.

Pham, J.R. Phillips, W.J. Shintler, P. Sheyko, and D.R. Tomash, The Polar plasma wave instrument, *Space Sci. Reviews, 71, 597, 1995.*

Harvey, P., F.S. Mozer, D. Pankiev, J. Wygant, N.C. Maynard, H. Singer, W. Sullivan, P. Il. Anderson, R. Pfaff, T. Aggson, A. Pedersen, C.-G. Fälthammer, and P. Tanskannen, The electric field instrument on the Polar satellite, Space *Sci. Revs.*, 71, 583, 1995.

Huba, J. D., N.T. Gladd, and J.F. Drake, On the role of the lower hybrid drift instability in substorm dynamics, *J. Geophys. Res.*, 86, 5881, 1981.

Johnson, J. R. and C. Z. Cheng, Global structure of mirror modes in the magnetosheath, *J. Geophys. Res.*, 102,7179, 1997.

Kennel, C. F., and H.E. Petschek, Limit on stably trapped particle fluxes, *J. Geophys. Res.*, 71, 1, 1966.

LaBelle, J., and R.A. Treumann, Plasma Waves at the dayside magnetopause, *Space Sci. Revs.*, 47, 175, 1988.

Lakhina, G. S., Low-frequency electrostatic noise due to velocity shear instabilities in the regions of magnetospheric flow boundaries, *J. Geophys. Res.*, 92, 12161, 1987.

Lakhina, G. S., Generation of low-frequency electric field fluctuations on auroral field lines, *Annales Geophysical, 64,660,* 1993.

Lakhina, G. S., P. K. Shukla, and L. Stenflo, Ultralow-frequency fluctuations at the magnetopause, *Geophys. Res. Lett.*, 20, 2419, 1995.

Lakhina, G. S., and B. Buti, Stochastic acceleration by lower hybrid waves in solar corona, *Solar Phys.*, 165,329, 1996.

Lakhina, G. S., B. T. Tsurutani, J. K. Arballo, C. M. Ho, and A. Boonsiriseth, Generation of broadband plasma waves in the polar cap boundary layer, *EOS, 78*, S297, 1997.

Peterson, W. K., Ion injection and acceleration in the polar cap, in *The Polar Cusp*, eds. J. A. Holtet and A. Egeland, D. Reidel Pub. Co., 63, 1985.

Pickett, J. S., R.R. Anderson, L.A. Frank, D.A. Gurnett, W.R. Paterson, J.D. Scudder, J.B. Sigworth, B.T. Tsurutani, C.M. Ho, G.S. Lakhina, W.K. Peterson, E. G. Shelley, C.T. Russell, G. K. Parks, M.J. Brittnacher, H. Matsumoto, K. Hashimoto, 1. Nagano, S. Kokubun, and T. Yamamoto, Correlative magnetopause boundary layer observations, *EOS,* 78, S291, 1997.

Rezeau, L., A. Morane, S. Perraut, A. Roux, and R. Schmidt, Characterization of Alfvénic fluctuations in the magnetopause boundary layer, *J. Geophys. Res.*, 94, 101, 1989.

Roy, M., and G.S. Lakhina, Lower hybrid wave model for aurora, *Astrophys. Space Sci., 117,* 111, 1985.

Russell, C. T., R.C. Snare, J.D. Means, D. Pierce, D. Dearborn, M. Larson, G. Barr and G. Le, The GGS/POLAR magnetic fields investigation, *Space Sci. Revs.*, 71, 563, 1995.

Shelley, E. G., A.G. Ghielmetti, H. Balsigar, R.K. Black, J.A. Bowles, R. P. Bowman, O. Bratschi, J.L. Burch, C.W. Carlson, A.J. Coker, J.F. Drake, J. Fischer, J. Geiss, A. Johnstone, D.L. Kloza, O.W. Lennartsson, A.L. Magoncelli, G. Paschmann, W.K. Peterson, H. Rosenbauer, T.C. Sanders, M. Steinacher, D.M. Walton, B.A. Whalen, and D.T. Young, The toroidal imaging mass-angle spectrograph (TIM AS) for the Polar mission, *Space Sci. Rev., 71*, 497, 1995.

Tsurutani, B. T., E.J. Smith, R.M. Thorne, R.R. Anderson, D.A. Gurnett, G.K. Parks, C.S. Lin, and C.T. Russell, Wave-particle interaction at the magnetopause: Contribution to the dayside aurora, *Geophys. Res. Lett., 8*, 183, 1981.

Tsurutani, B. T., and R.M. Thorne, Diffusion processes in the magnetopause boundary layer, *Geophys. Res. Lett., 22, 663,* 1982.

Tsurutani, B. T., A.L. Brinca, E.J. Smith, T. Okuda, R.R. Anderson, and T.E. Eastman, A survey of ELF-VLF plasma waves at the magnet topause, *J. Geophys. Res.*, 94, 1270, 1989.

Tsurutani, B. T., D. J. Southwood, E.J. Smith, and A. Balogh, A survey of low-frequency waves at Jupiter: The Ulysses encounter, *J. Geophys. Res.,* 98,21203, 1993.

Tsurutani, B. T., and W.D. Gonzalez, The efficiency of "viscous interaction" between the solar wind and the magnetosphere during intense northward IMF events, *Geophys. Res. Lett., 22,663,* 1995.

Tsurutani, B. T., J. K. Arballo, B.E. Goldstein, C.M. Ho, G. S. Lakhina, E.J. Smith, N. Cornilleau-Wehrlin, R. Prange, N. Lin, P. Kellogg, J.L. Phillips, A. Balogh, N. Krupp and M. Kane, Plasma wave characteristics of the Jovian magnetopause boundary layer: Relationship to the Jovian aurora?, *J. Geophys. Res.*, 102,4751, 1997.

Zhu, Z., P. Song, J.F. Drake, C.T. Russell, R.R. Anderson, D.A. Gurnett, K.W. Ogilvie, and R.J. Fitzenreiter, The relationship between ELF-VLF waves and magnetic shear at the dayside magnetopause, *Geophys. Res., Lett.,* 23,773, 1996.

Figure Captions

Figure 1. POLAR orbit and the region of wave detection (solid bar) in the magnetosphere. POLAR has a perigee at 1.8 R_E and apogee at 9 R_E. Waves on the field lines that map into the low latitude boundary layer (LLBL) are the topic of this study.

Figure 2. A schematic of the Polar spacecraft showing the orientation of the three orthogonal electric antennas (E_u, E, and E_Z), the magnetic loop antenna (B_L), and the triaxial search coil antennas (B_u, B_v, and B_Z).

Figure 3. Color spectrogram of wave electric field from -101 to 10^4 Hz and above. The boundary layer waves are indicated. In between the two boundary layer (dayside and nightside) crossings is the polar cap (quiet wave region).

Figure 4. Occurrence frequency of northern dayside PCBL waves as a function of local time. The polar cap boundary layer waves are present on the dayside nearly 100% of the time (05- 18 LT). The statistics are listed on the top.

Figure 5. a) The geomagnetic latitude of the footpoint of the B field line passing through the spacecraft versus local time (GMT). Regions of wave activity are primarily located on the field lines whose footpoint geomagnetic latitudes lie between 70°-80°. b) L-value distribution of the PCBL waves versus GMT. The wave region is located for $L \geq 10$.

Figure 6. The electric field a) and magnetic field b) spectra for the events occurring on Day 098, 1996. The background noise is indicated. The electric waves extend beyond the electron cyclotron frequency (-6 x 10^3 Hz).

Figure 7. The electric field a) and magnetic field b) spectra for the event occurring on Day 114, 1996. The background noise is indicated. The electron cyclotron frequency is indicated, The electric waves extend beyond the electron cyclotron frequency (-7 x 10^3 Hz).

Figure 8. Wide band high time resolution plot for the PCBL wave event on Day 114, 1996. The waves are very spiky and highly variable in intensity.

Figure 9: The B′/E′ ratio for two events, one on day 98 (panel a) and the other on day 114 (panel b). The whistler wave refractive index is also shown. These ratios are highly variable but lie between the values 10 to 100. For parallel propagating whistler modes, the ratio B'/E' should fall off with frequency with a $f^{-1/2}$ dependence.

Figure 10. Color spectrogram of the H+, 0', He^{+} and He^{++} ion fluxes observed by the TIMAS experiment (top 4 panels) and the electric component of the PWI broadband plasma wave event (lower panel) on day 98, 1996.

Figure 11. Color spectrogram of the ion fluxes and waves observed on day 113, 1996. The format is the same as in Figure 10.

Figure 12. A northern polar view of the mapping of polar cap boundary layer (PCBL) waves to the low latitude boundary layer (LLBL).

Table Captions

Table 1. A comparison of POLAR broadband plasma wave properties and past observations from ISEE and GEOS. The wave intensities and the spectral shapes are similar on POLAR and ISEE. The reason for higher wave intensities on GEOS are discussed in the text.

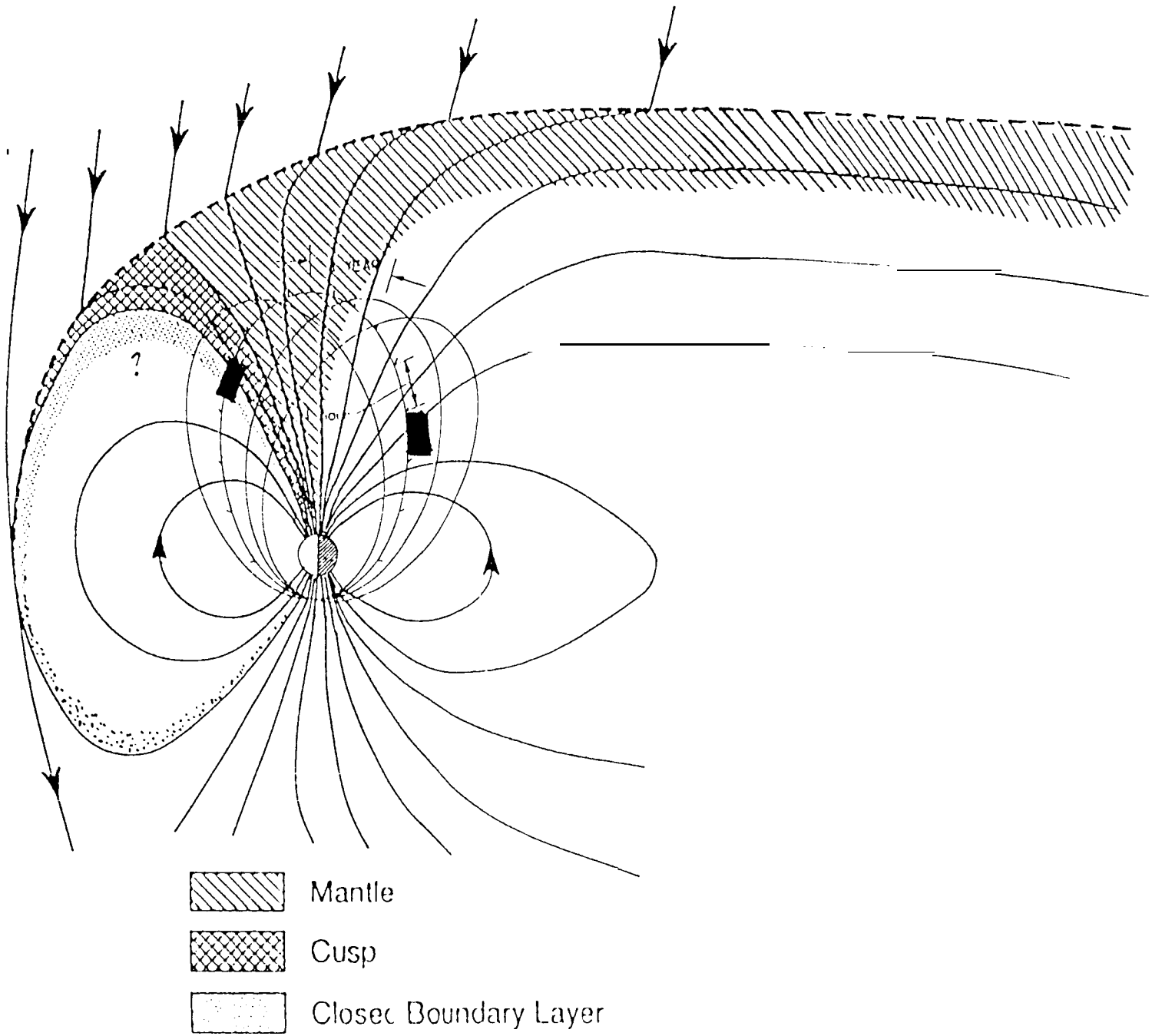

Fig 1

A-G92-27-3

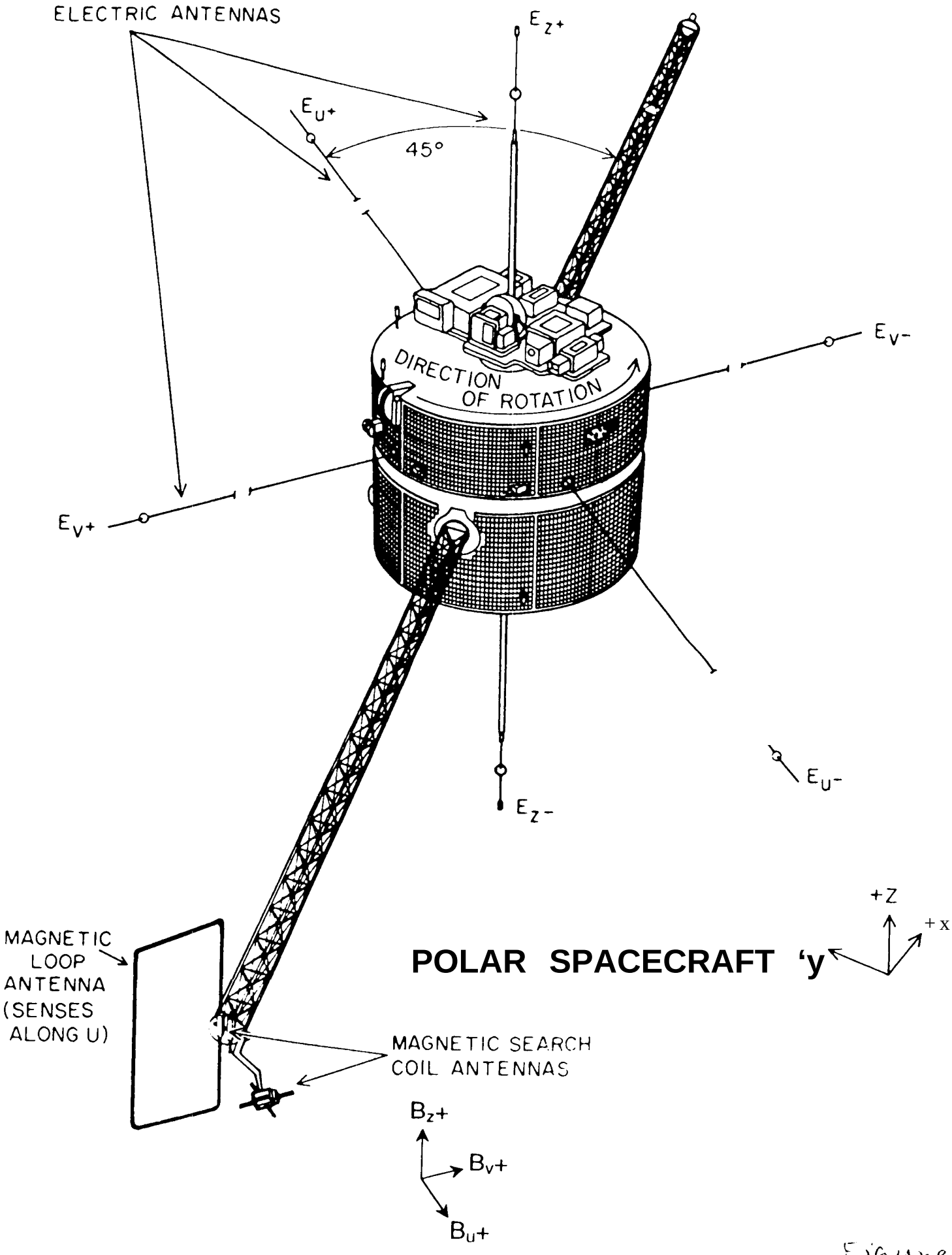

POLAR SPACECRAFT 'y

Figure 2

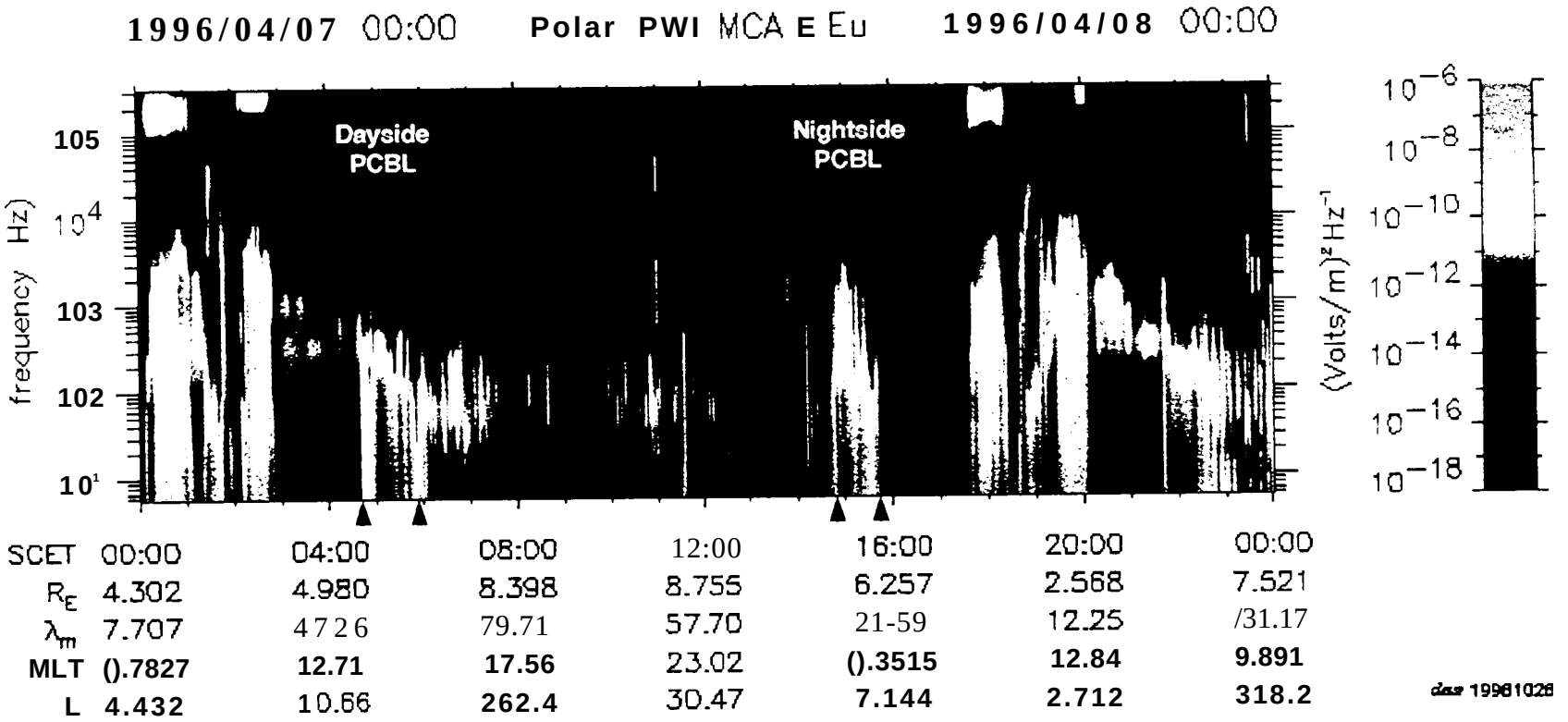
1996/04/07 00:00
Polar PWI MCA E Eu
1996/04/08 00:00
Dayside PCBL
Nightside PCBL
frequency Hz)
105
10^4
103
102
10^1
(Volts/m)^2 Hz^-1
10^-6
10^-8
10^-10
10^-12
10^-14
10^-16
10^-18
SCET 00:00 04:00 08:00 12:00 16:00 20:00 00:00
R_E 4.302 4.980 8.398 8.755 6.257 2.568 7.521
λ_m 7.707 4726 79.71 57.70 21-59 12.25 /31.17
MLT ().7827 12.71 17.56 23.02 ().3515 12.84 9.891
L 4.432 10.66 262.4 30.47 7.144 2.712 318.2
das 19981028

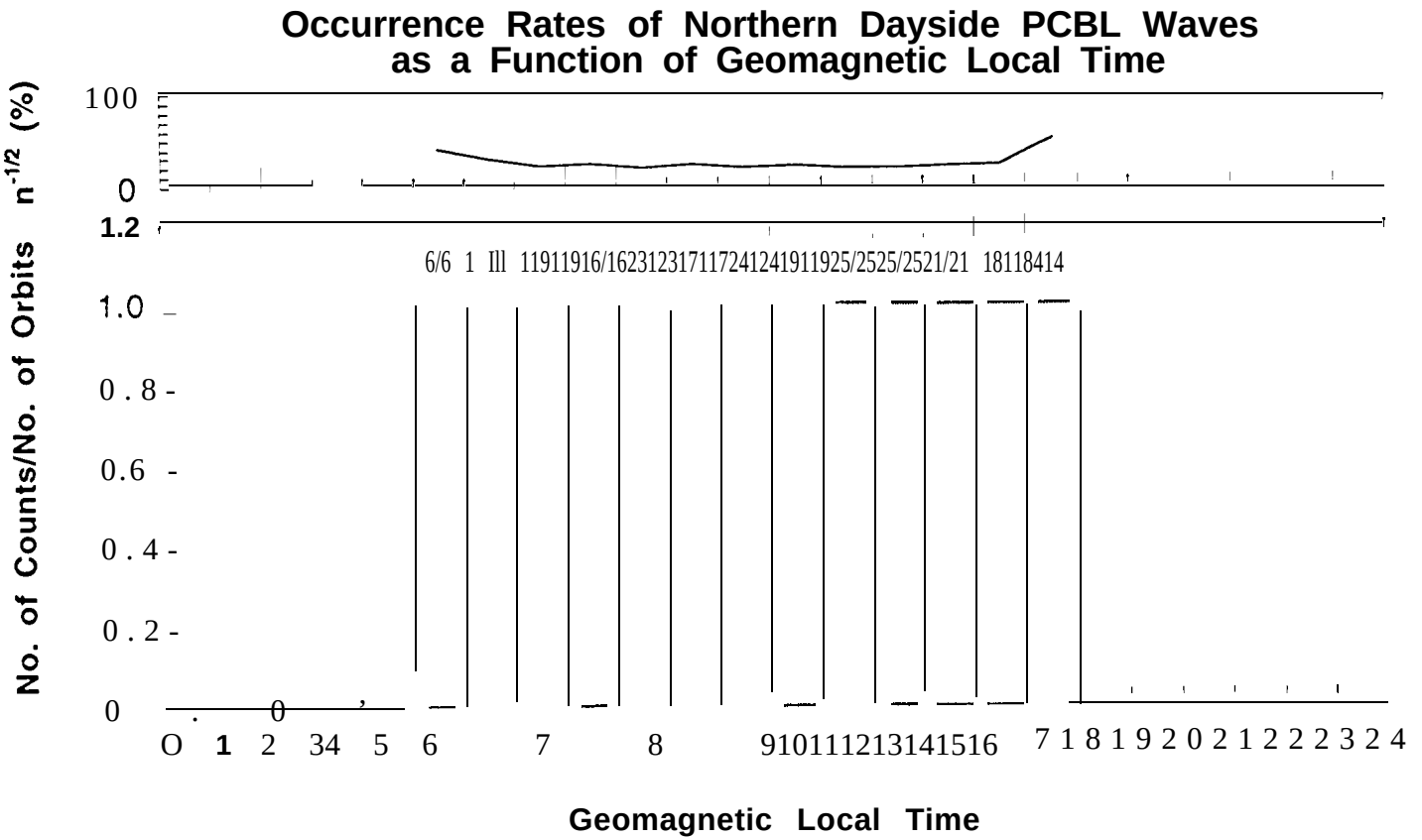
Occurrence Rates of Northern Dayside PCBL Waves
as a Function of Geomagnetic Local Time
No. of Counts/No. of Orbits n-1/2 (%)
100
0
1.2
6/6 1 Ill 11911916/16231231711724124191192525/2525/2521/21 18118414
1.0
0.8
0.6
0.4
0.2
0
O 1 2 34 5 6 7 8 910111213141516 7 1 8 1 9 2 0 2 1 2 2 2 3 2 4
Geomagnetic Local Time

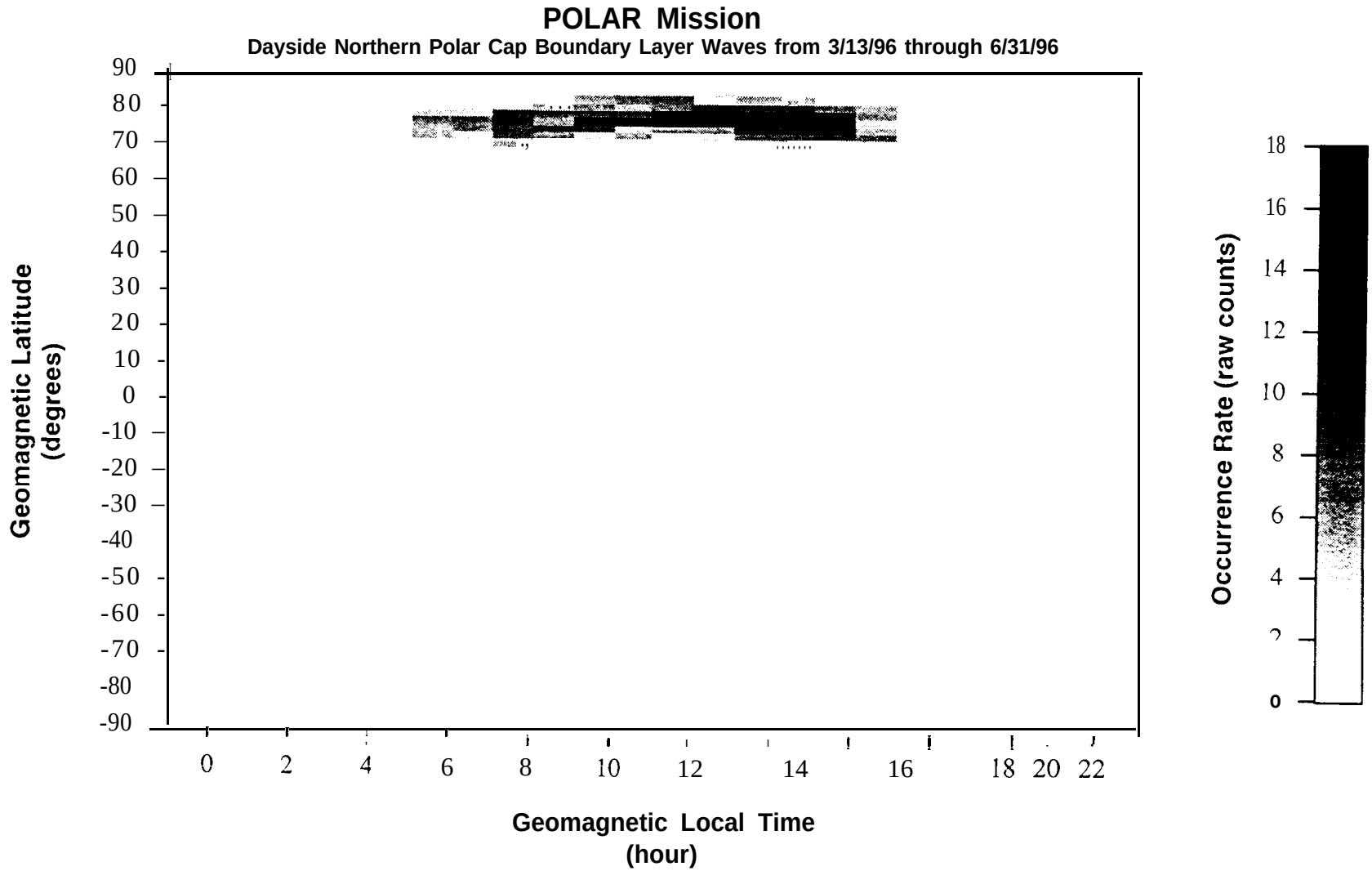
POLAR Mission
Dayside Northern Polar Cap Boundary Layer Waves from 3/13/96 through 6/31/96
Geomagnetic Latitude (degrees)
90
80
70
60
50
40
30
20
10
0
-10
-20
-30
-40
-50
-60
-70
-80
-90
0
2
4
6
8
10
12
14
16
18
20
22
Geomagnetic Local Time (hour)
Occurrence Rate (raw counts)
18
16
14
12
10
8
6
4
2
0

Fig 5a

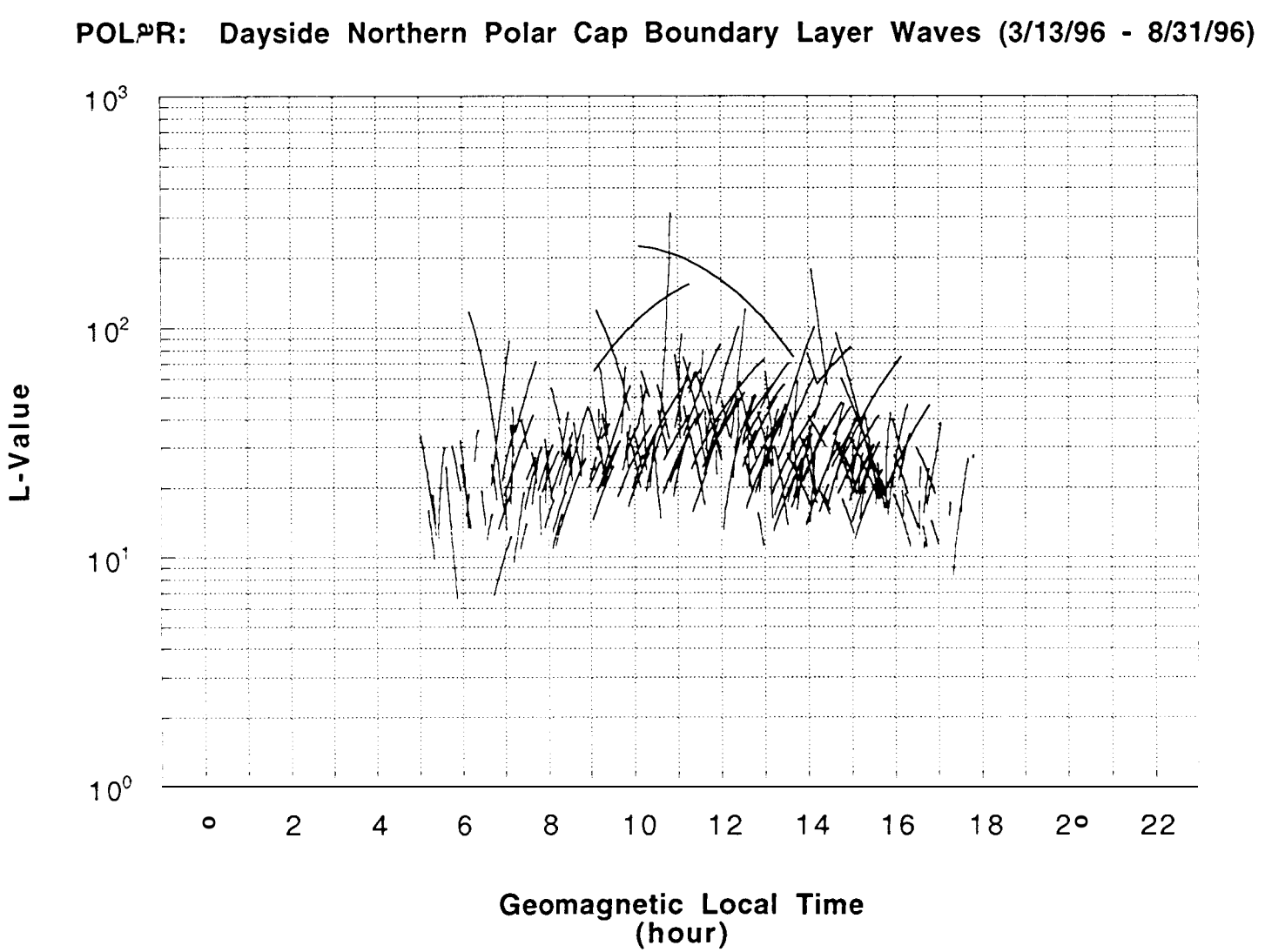
POLAR: Dayside Northern Polar Cap Boundary Layer Waves (3/13/96 - 8/31/96)
L-Value
10^3
10^2
10^1
10^0
0
2
4
6
8
10
12
14
16
18
20
22
Geomagnetic Local Time
(hour)

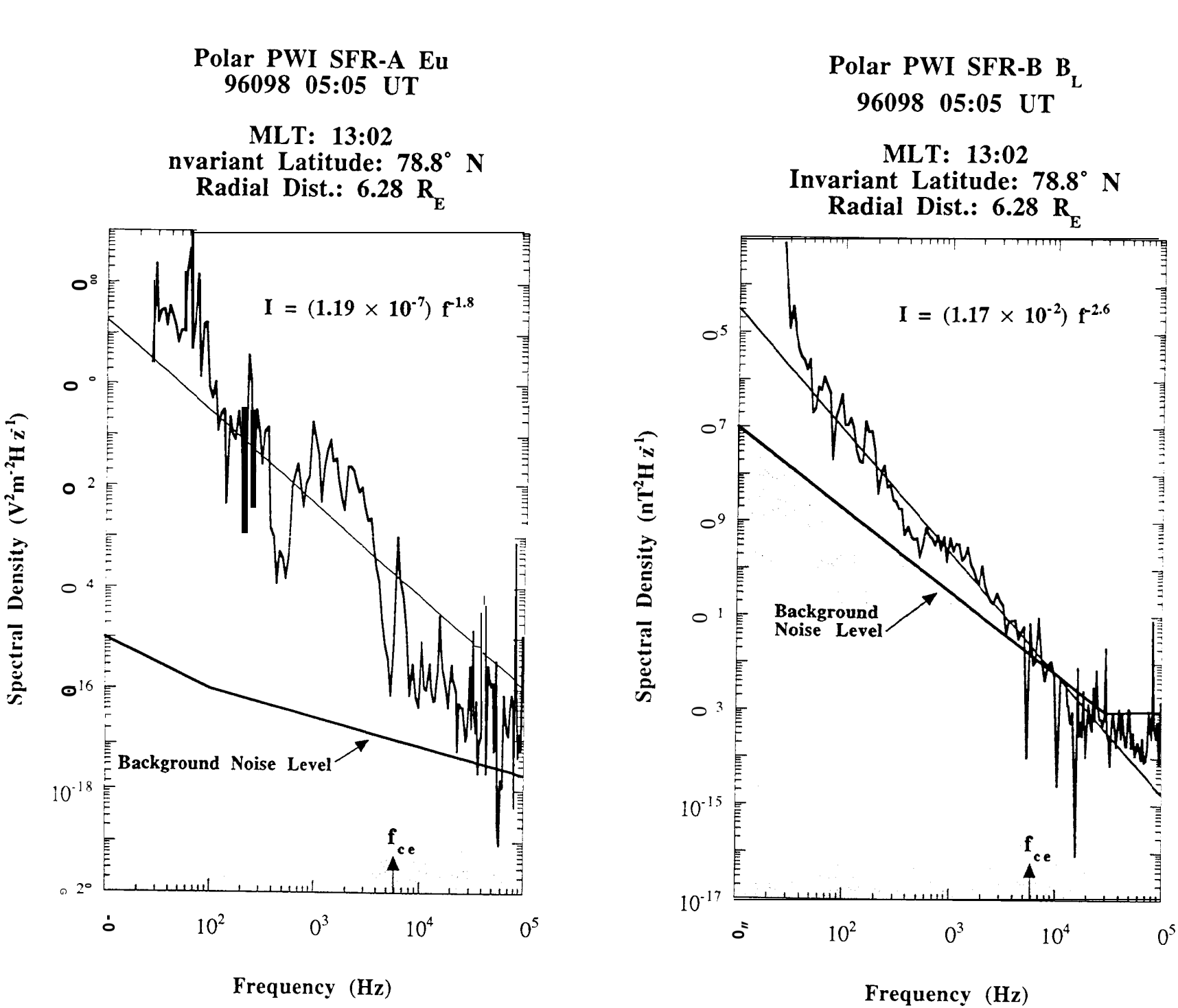
Polar PWI SFR-A Eu
96098 05:05 UT
MLT: 13:02
nvariant Latitude: 78.8° N
Radial Dist.: 6.28 R_E
I = (1.19 × 10^-7) f^-1.8
Background Noise Level
f_ce
Spectral Density (V²m⁻²Hz⁻¹)
Frequency (Hz)
Polar PWI SFR-B B_L
96098 05:05 UT
MLT: 13:02
Invariant Latitude: 78.8° N
Radial Dist.: 6.28 R_E
I = (1.17 × 10^-2) f^-2.6
Background Noise Level
f_ce
Spectral Density (nT²Hz⁻¹)
Frequency (Hz)

Figure 6

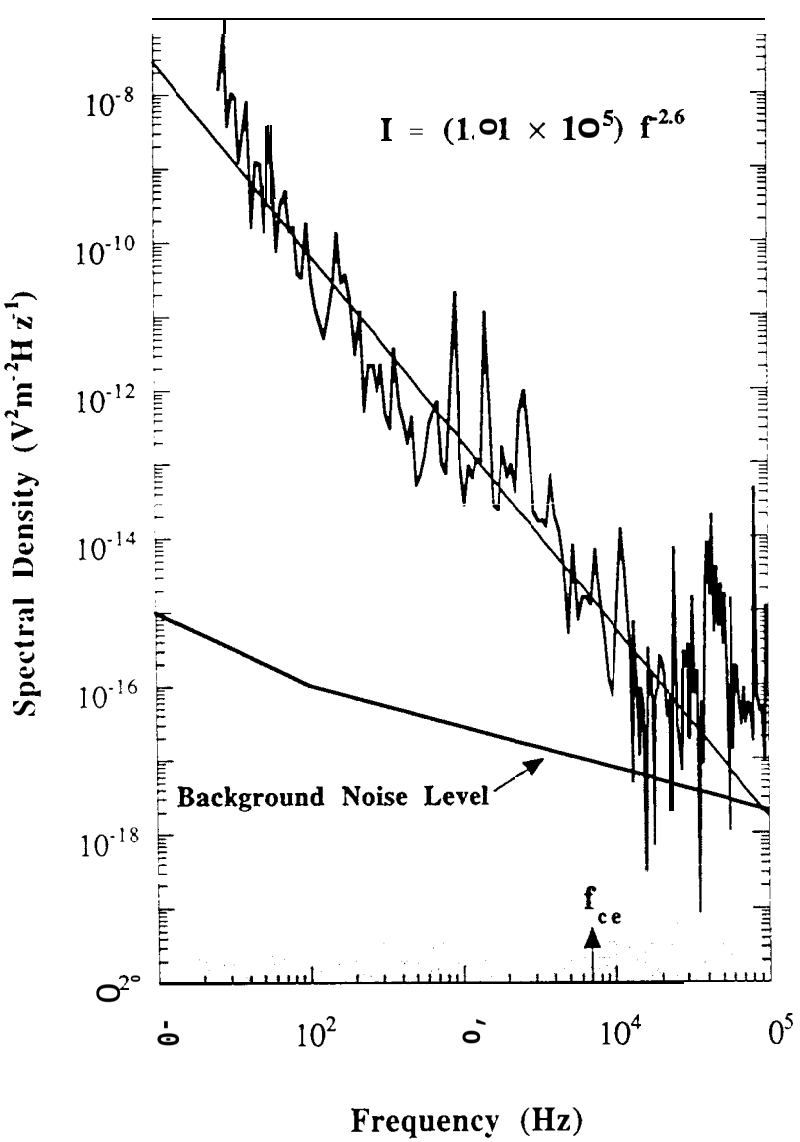
Polar PWI SFR-A Eu
96114 06:33 UT
MLT: 12:35
Invariant Latitude: 76.3° N
Radial Dist.: 5.82 R_E
I = (1.01 × 10^5) f^-2.6
Background Noise Level
f_ce
Spectral Density (V²m⁻²H z⁻¹)
Frequency (Hz)

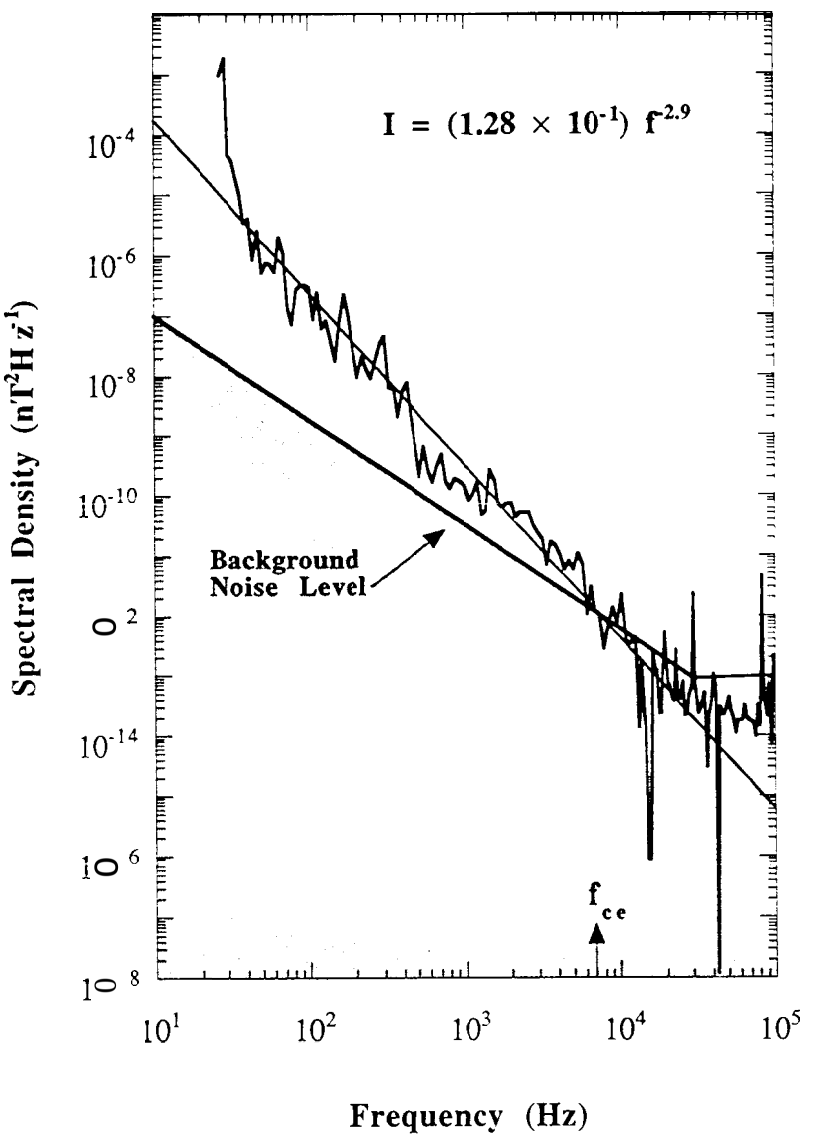
Polar PWI SFR-B B_L
96114 06:33 UT
MLT: 12:35
Invariant Latitude: 76.3° N
Radial Dist.: 5.82 R_E
I = (1.28 × 10^-1) f^2.9
Background Noise Level
f_ce
Spectral Density (n'T²H z⁻¹)
Frequency (Hz)

Figure 7

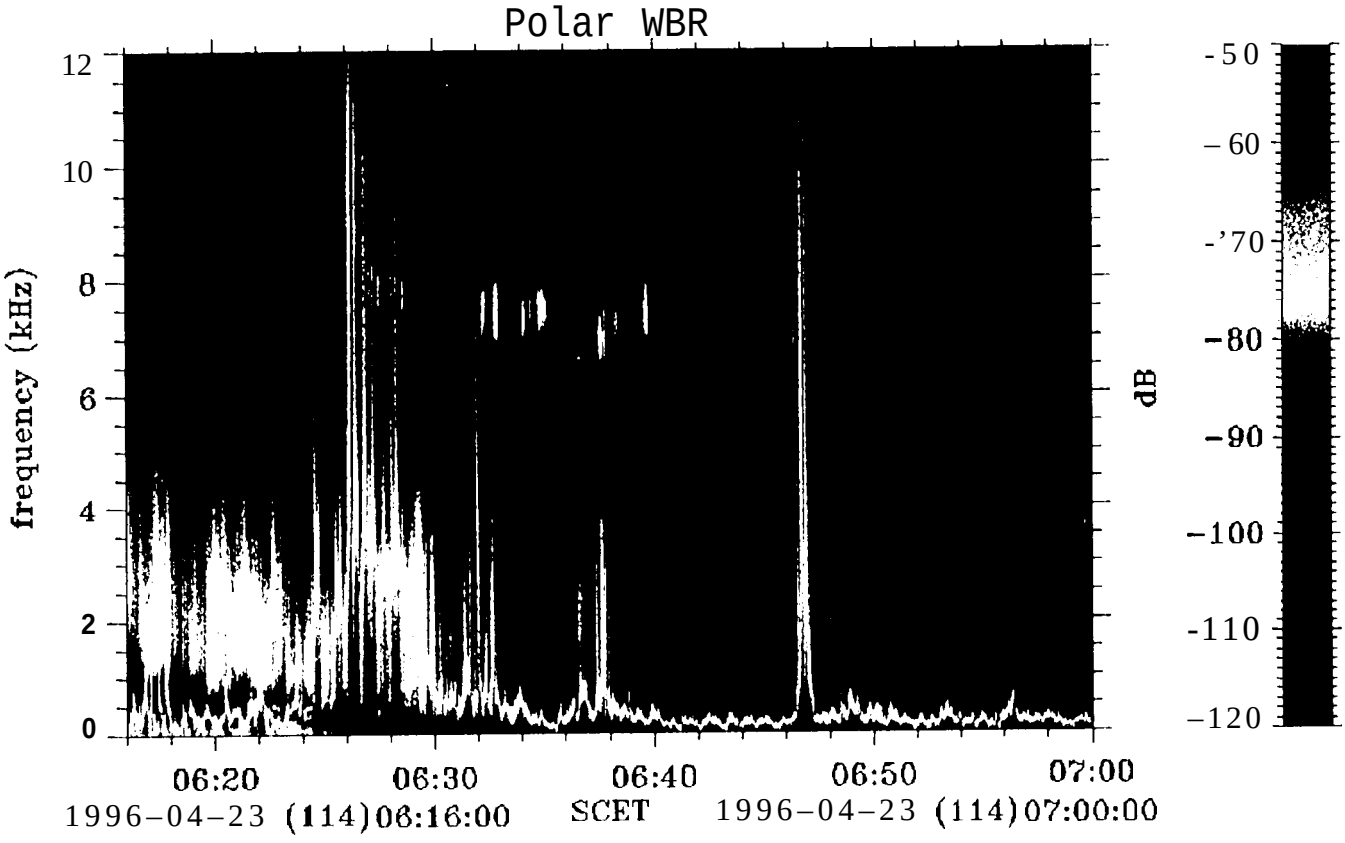
Polar WBR
frequency (kHz)
12
10
8
6
4
2
0
dB
-50
-60
-70
-80
-90
-100
-110
-120
06:20
06:30
06:40
06:50
07:00
1996-04-23 (114)06:16:00 SCET 1996-04-23 (114)07:00:00

Figure 8

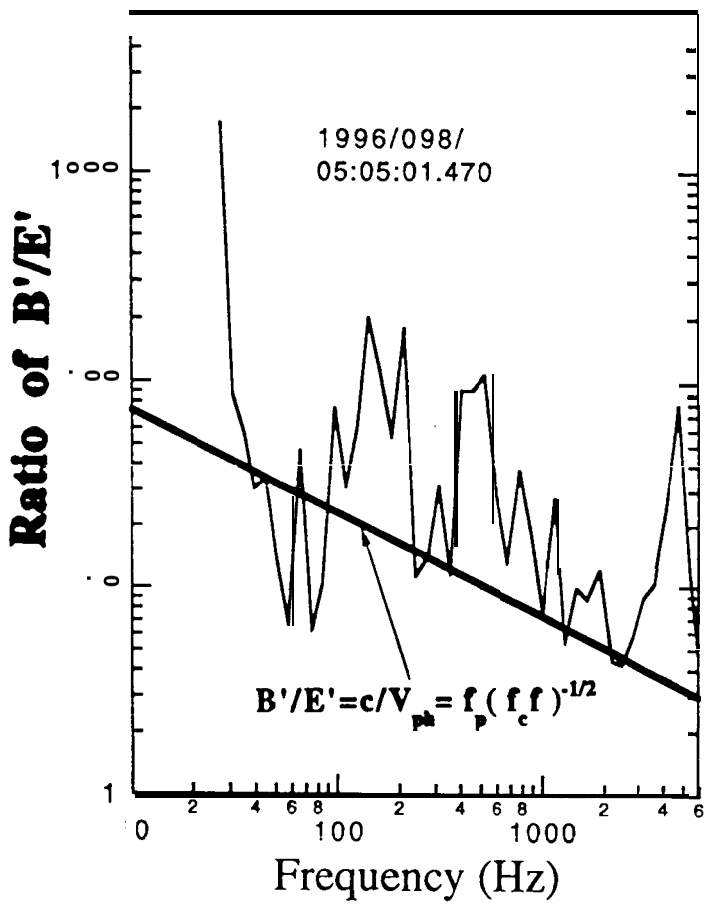
1996/098/
05:05:01.470
Ratio of B'/E'
B'/E'=c/V_ph= f_p(f_c f)^-1/2
Frequency (Hz)

a)

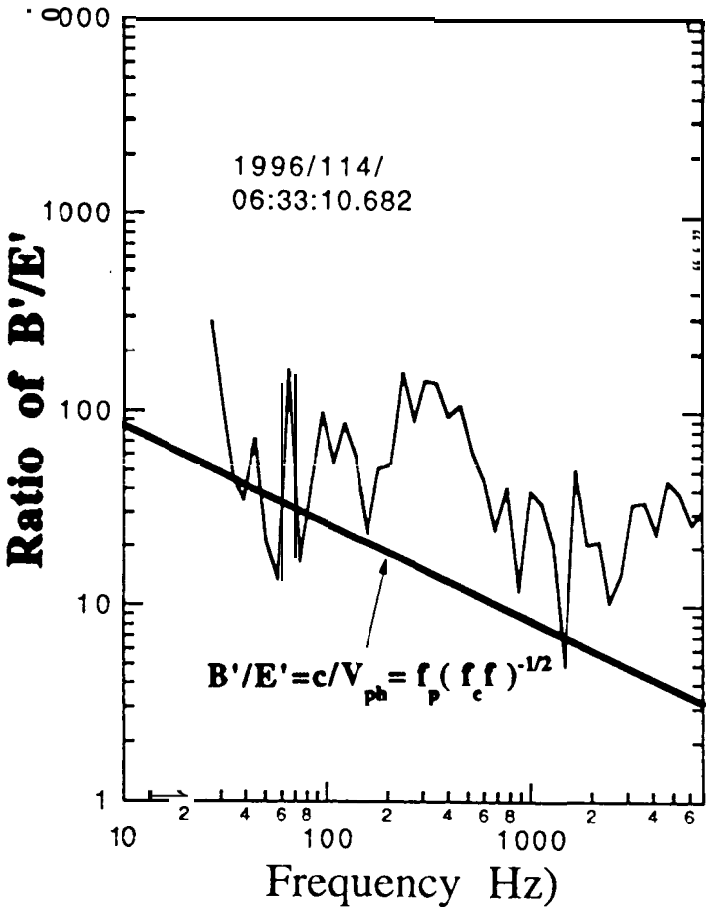
1996/114/
06:33:10.682
Ratio of B'/E'
B'/E'=c/V_ph= f_p(f_c f)^-1/2
Frequency Hz)

b)

Fig 9

Polar - Apr 7, 1996 (96098)

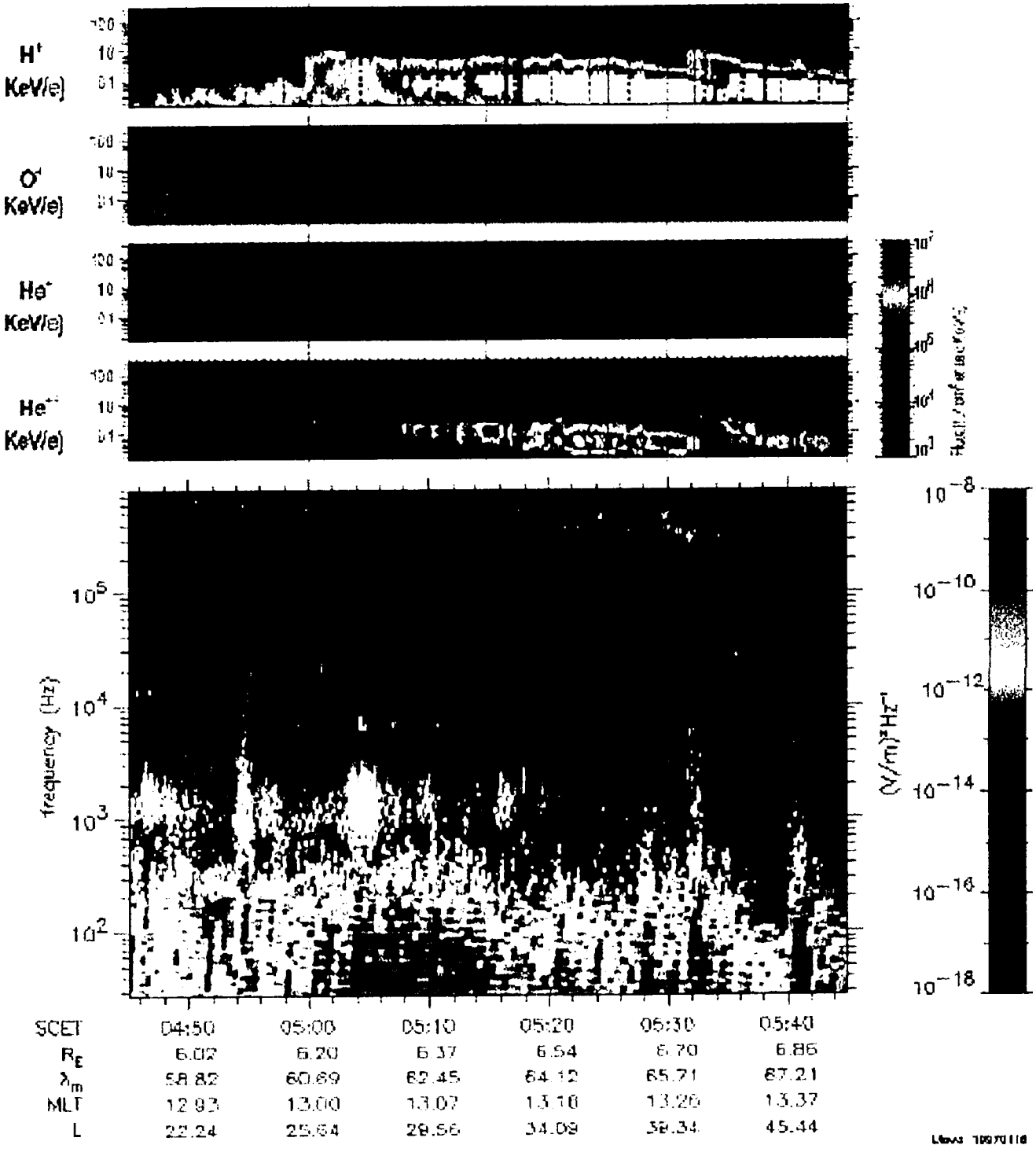

Polar - Apr 22, 1996 (96113)

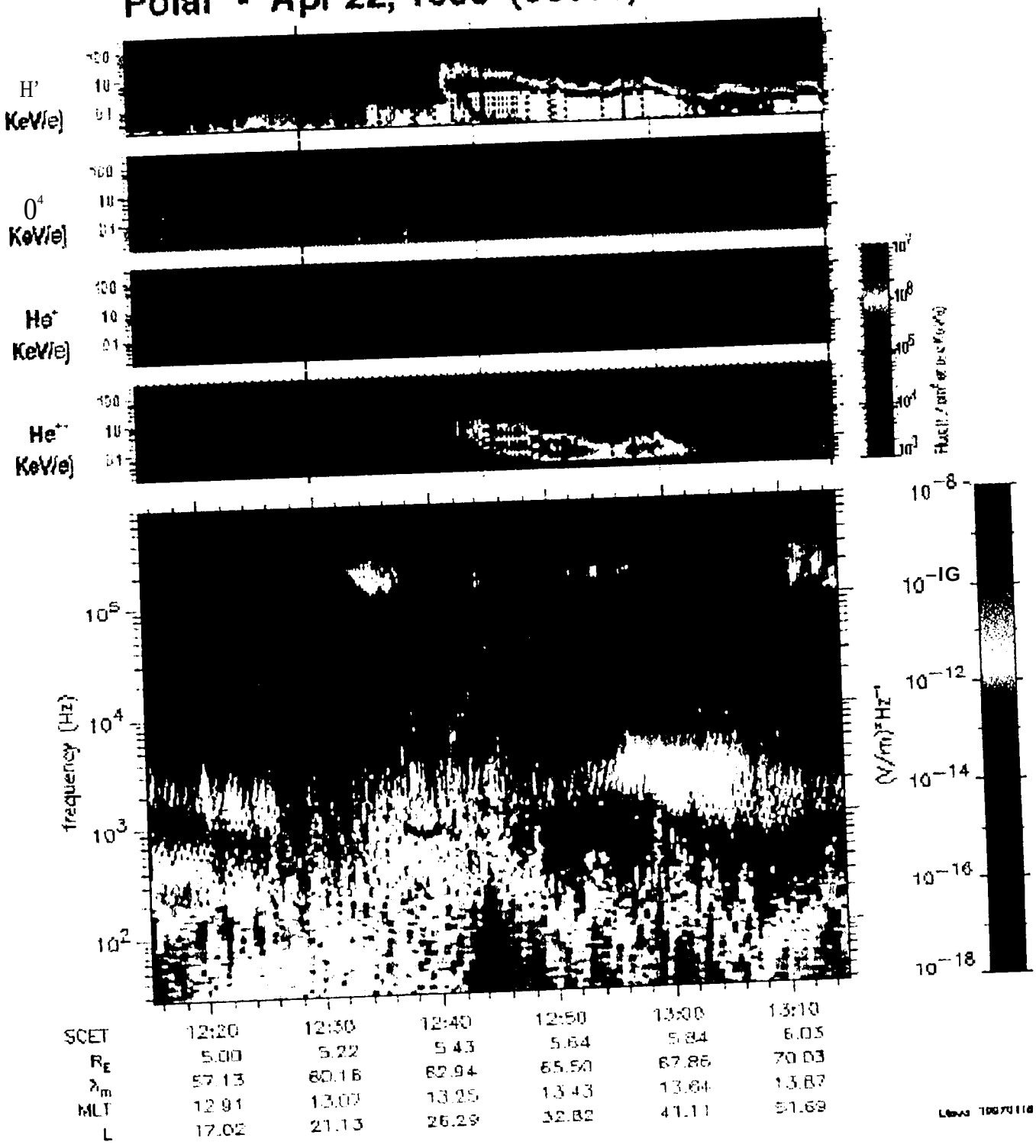

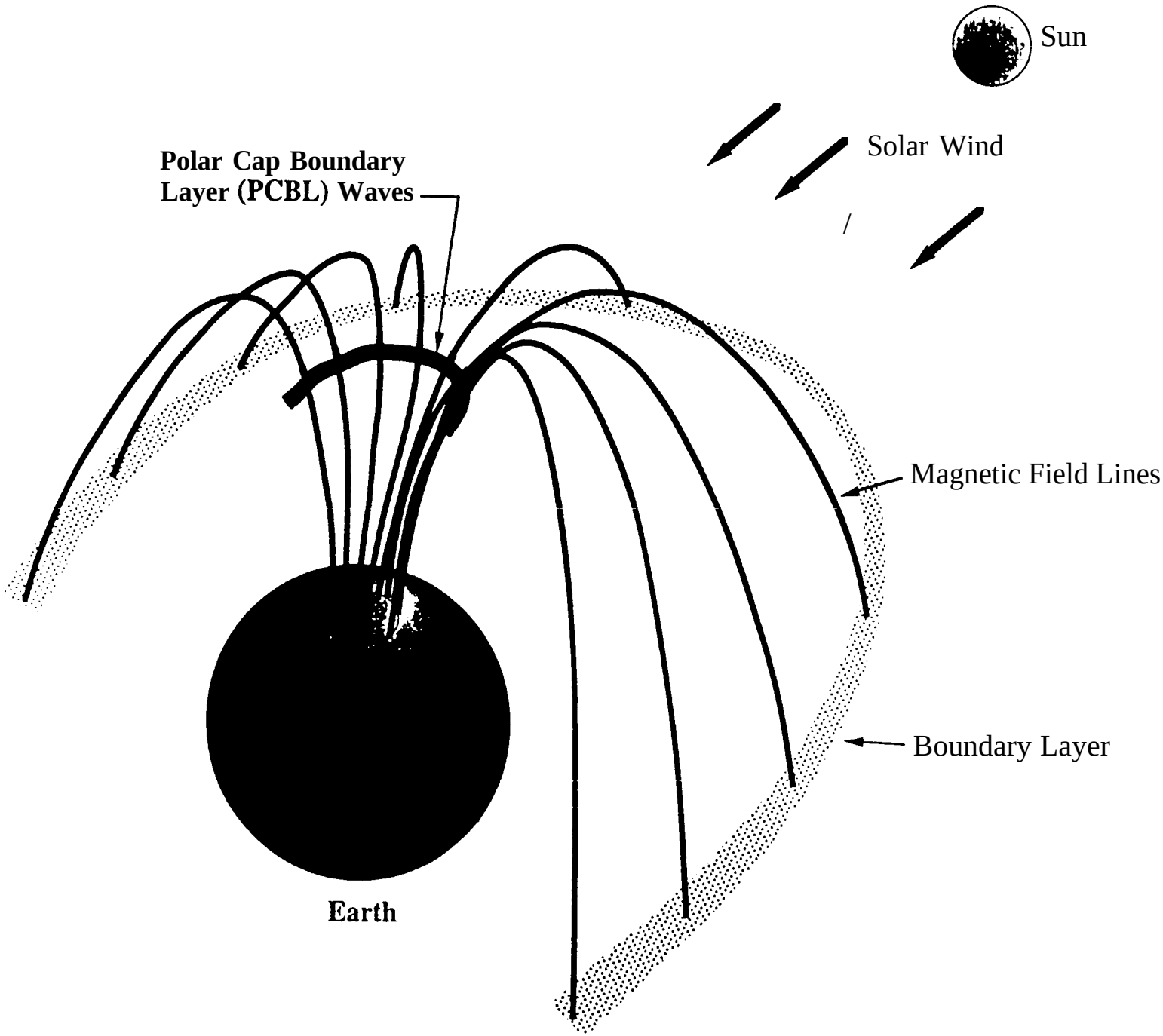
Sun
Solar Wind
Polar Cap Boundary Layer (PCBL) Waves
Magnetic Field Lines
Boundary Layer
Earth

Fig. 12

Spacecraft	Location	Date	B' (nT) 2 /Hz	E' (V/m) 2 /Hz
POLAR (this paper)	**-7-8** R_E altitude	day 098, 1996	(1.17 X1O-2) f -2.6	(1.19×10^{-7}) f -1.8
	-2RE altitude	day 103, 1996	(1 .34x 10^{-2}) f -2.5	(1.22X 10^{-6}) f -1.8
ULYSSES *Tsurutani et a/. [1995]*	Jupiter magnetosphere	day 043, 1992	(2.0×10^{-4}) f -2.4	(4.0 x 10^{-9}) f -2.4
ISEE 1 *Gurnett et al. [1979]*	Earth's magnetopause	day 314, 1977	~ f -3.3	~f -2.2
ISEE 1 and 2 *Tsurutani et al. [1981]*	Earth's magnetopause	1977	(1×10^{1}) f -3.9	**(3X 1o-5)** f -2.8
ISEE 1 and 2 *Anderson et al. [1982]*	Earth's magnetopause	1977	(7.9 x 1 0^{-2}) f -2.9	(6.3 *X 10-6)* f -2.2
GEOS **2** *Rezeau et al. [1989]*	Earth's magnetopause	day **240, 1978**	**(3.6x** 10^{1}) **f** -2.6	**(1.2** x **10-6) f** -2.6
ISEE 1 *Tsurutani et al. [1989]*	Earth's magnetopause	1977-1978	(3x 10^{-1}) f -3.3	(6X **10-7) f** -2.1

Table 1: